



## Simulation of Soil Organic Carbon Dynamics in Oasis Farmland in Xinjiang based on DNDC model

DONG-LIANG HAN<sup>1,3</sup>, XIN-JUN WANG<sup>1,3</sup>, XIN-PING ZHU<sup>1,3</sup>, HONG-TAO JIA<sup>1,3</sup> AND CHENG-YI ZHAO<sup>2</sup>

<sup>1</sup>College of Grassland and Environmental Sciences, XinJiang Agricultural University, Urumqi 830052, China;

<sup>2</sup>XinJiang Institute of Ecology and Geography, Chinese Academy of Sciences, Urumqi 830011, China;

<sup>3</sup>Xinjiang Key Laboratory of Soil and Plant Ecological Processes, College of Grassland and Environmental Sciences, Xinjiang Agricultural University, Urumqi 830052, China

Email: jiahongtao2015@126.com, donglianghan555@126.com

**Abstract:** This paper reports a study of long-term fertilization impacts on soil organic carbon (SOC) dynamic using DNDC (denitrification-decomposition) model to simulate the related experimental parameters in Manas Country, Xinjiang province. RMSE, M, and R values were used to verify the DNDC model. Meanwhile, the simulation predicted that fertilizer (N+P+K+S, plant residue returned) treatment and the trend of SOC in the different soil types, and analysis of corresponding  $\Delta$ SOC and the initial value in soil chemical and physical properties. In addition, based on GIS the spatial distribution was calculated by SOC content, bulk density, depth, density of soil carbon conversion (SOCD). Results showed that through DNDC model simulation SOC increased 1.9g kg from 2011 to 2041 year; soil carbon density ranges from 0.012kg C m<sup>-1</sup> to 0.021 kg C m<sup>-1</sup>. Soil carbon sequestration rate ranges from 807 kg ha<sup>-1</sup> yr<sup>-1</sup> to 121kg C ha<sup>-1</sup> yr<sup>-1</sup>. Carbon density of the Manas country farmland was increasing. Moreover, high SOC content has higher sequestration rate than low SOC content.

**Keywords:** Soil organic carbon; DNDC model; GIS; Grey desert soil; Manas country

### 1. Introduction

Soil organic carbon (SOC) is one of the most important terrestrial pools for storage [1-2]. Even very small local changes of the SOC pool may potentially add up to significant changes in large-scale carbon (C) cycling [3]. It is estimated that the total SOC pool is about 1400500 Pg C (1Pg=10<sup>15</sup>g), which is approximately two times greater than the atmospheric pool (750 Pg) [4-6]. SOC is one of the key factors that affect agricultural production, nutrient availability, soil stability and the flux of greenhouse gases between land surface and atmosphere [7]. SOC represents a major pool of carbon within the biosphere, and acts both as a source and a sink for carbon. Variation of SOC reflects the net result of additions of [11]. Zhang [14] reported that the changes of fertilizer carbon and the carbon loss of SOC may cause quantity used in Xinjiang for 15 years have been soil degradation, which does not only undermine sustainable agricultural development but also affects environmental health [7]. Consequently, improved management practices should aim to increase SOC accumulation, as these practices affect both world food security and global climate change [8-9].

Estimates from the IPCC Second Assessment Report suggested that 40000 Tg (1Tg=10<sup>12</sup>g) C per year could be sequestered in global agricultural soils, with the finite capacity saturating after 50100 years [10]. Sun [11] suggested that the potential of SOC sequestration in China was estimated to be 25 Pg C, which could be achieved by the 2050 crop production and field management are improved.

Smith [12] reported the biological potential for carbon storage in European (EU15) cropland to be 120 Tg C per year with the available management options including reduced and zero tillage, ~~side~~ (i.e., land that farmers are not allowed to use for any agricultural purpose), and the more efficient use of organic amendments. Sperow [13] further projected that U.S. cropland has the potential to increase soil C sequestration by an additional 70 Tg C yr<sup>-1</sup> over the rate of 17 Tg C yr<sup>-1</sup> in the early 2000s.

Over the past 30 years, croplands in China have approximately doubled as a result of the adoption of modern cultivars, the increased use of fertilizer, improved field management, and expanded irrigation. Variation of SOC reflects the net result of additions of [11]. Zhang [14] reported that the changes of fertilizer carbon and the carbon loss of SOC may cause quantity used in Xinjiang for 15 years have been soil degradation, which does not only undermine sustainable agricultural development but also affects environmental health [7]. Consequently, improved management practices should aim to increase SOC accumulation, as these practices affect both world food security and global climate change [8-9].

The vast majority of the changes in the SOC are believed to occur in the top 20 cm of soil [15-17], the changes within an additional 20 cm depth are well understood, which may result in an appropriate assessment of the soil carbon sequestration.

The spatial and temporal characteristics of soil C describe are difficult to determine in limited field experiments. Therefore, it is required to establish a comprehensive process-based model of simulating such a complex process and deriving management

practices to soil describe [18]. A list of the most widespread models to simulate SOC storage and loss from cropland under global warming scenarios were as follows: NCSOIL [19], CENTURY [20], RothC [21], LEACHM [22] and DNDC [23-24]. The DNDC model is one of the few models developed including both a site-specific mode and a regional mode, simulating carbon biogeochemistry in agro ecosystems, is used to study the agricultural soils of China. Moreover, the DNDC model has been validated throughout the world by using long-term and short-term experimental data, testing the modeling behavior and sensitivity of the carbon biogeochemical process in agricultural soils [25-27]. Nowadays, the DNDC model has been modified and improved by adding new function. Meanwhile, DNDC was also reported to a good performance models by using fertilization experiments representing oasis land uses, a range of climatic conditions within the arid region, and fertilization treatments [28-29].

Xinjiang province in northwest China is a unique region with strong geographical heterogeneity and complex meteorological systems [30-33]. In Xinjiang, several studies have reported SOC on a local scale agricultural [34-35]. Nationwide studies have been conducted by analyzing the large number of different soil profiles found in the literature. However, several limitations exist: these records generally result from observations made with data obtained from various sources; the values obtained in samplings done in different years are mixed; and the data obtained from different approaches have led to wide variations. In the present work, we assess SOC, bulk density (BD) and stoniness spatial variability as edaphic attributes in Xinjiang soils.

This paper presents an approach to estimate the carbon density in Manasi county, Xinjiang province using soil quality data (1 study plots) and simple geostatistical technique for evaluation purposes. The objectives of this study were to: (1) quantify current SOC and soil organic carbon density (SOCD) in Manas county, Xinjiang and (2) generate fine resolution estimates of surface soil SOC stocks from 2011 to 2041, reveal the spatiotemporal pattern of the regional C pools, and assess the best reasonable fertilization factors mainly in the grey desert soil at the arid or semiarid regions of Northwest China.

## 2. Materials and Methods

### 2.1. Study Area

The study area is located in northwest China, Manas county, Xinjiang province, (N43°28'-45°38', E85°34'-86°43') covering about an agricultural acreage of 700 km<sup>2</sup> (Fig. 1).

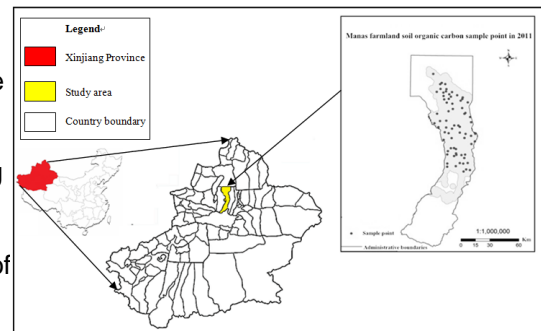


**Fig. 1** Location of the study area in China and monitoring sites and County in the study area.

The climate is arid or semiarid with full of sunshine. Annual average rainfall is 173.3 mm, with a mean temperature of 7.7 °C. There is a rotation of corn wheat/cotton (i.e., corn and cotton cropping for one year and wheat cropping for next two year) in the local. Corn was seeded during late April to early May for the monocropping system. Spring wheat was seeded in mid-April and winter wheat in late September in the same year. Cotton was seeded in May in the year. According to farmer surveys in 2011, chemical fertilizer was commonly used as its application is less laborious than that of manure. In the wheat growing season, nitrogen fertilizer was commonly applied before sowing. Similar applications of nitrogen fertilizer were used for cotton before sowing. In the corn growing season, nitrogen fertilizer was commonly applied in the days between node elongation and tasseling. Drip irrigation was widespread. Wheat fields were commonly irrigated three to four times, corn fields one or two times, and cotton was commonly irrigated two to three times. General characteristics of the sites are shown in Table 1.

**Table.1** Basic soil information (mean±S.D.) of the topsoil samples

Soil types	No. of samples	Area (10 <sup>4</sup> ha)	Mean initial SOC (g kg <sup>-1</sup> )	Bulk density (g cm <sup>-3</sup> )	pH values
Meadow Soil	7	1.64	6.98±0.35	1.34	8.38
Gray desert soi	27	6.92	7.31±0.74	1.46	8.43
Moisture soil	12	3.22	8.73±1.26	1.23	8.48
Aeolian sandy soi	7	1.38	4.24±0.67	1.41	8.33
Irrigated desert soils	2	0.27	6.24±0.73	1.44	8.18
Desert solonchak	6	1.28	8.21±1.22	1.34	8.61
Shrubby meadow soils	2	0.41	7.86±0.11	1.39	8.28

Alluvial soils	2	0.33	10.18±0.51	1.29	8.37
Solonchak	6	1.14	6.87±0.59	1.38	8.59
All/Mean	71	16.59	7.40±0.69	1.36	8.41

## 2.2. Soil Sample and Analyses

In August and September 2012, based on the practical conditions and employing Global Position System (GPS), 71 sampling points were located with every three random topsoil (20cm) samples from each sampling point mixed together for chemical analysis. Soil samples were stored in cloth bags, transported to the laboratory and air dried at room temperature. Then the soils were crumbed, and passed through a 2 mm mesh to remove visibly identifiable plant residues, fauna, and debris. Generally, the soils were nearly stone free and we did not measure soil stone content. A small fraction of each sample was ground and passed by a 0.25 mm mesh for analyses of SOC concentrations. SOC was determined using the  $K_2Cr_2O_7-H_2SO_4$  oxidation method [36]. Soil bulk density (BD) of sampling site was measured using the core method described by Ale and Hartage [37]. Soil BD samples were dried at 105 °C until a constant mass and weighed to calculate BD by dividing by soil volume. The pH (soil water suspensions, 1:2.5) was measured using the PHC instrument (INESAS Scientific Instrument Co., Ltd) Particle size distribution, one of the basic physical properties of soil, can be used to calculate other characteristic parameters of the soil. Though time consuming, the densimeter method is the common way to determine particle-size distribution of fine grain soils [38]. Soil total N (TN) and Soil total P (TP) contents were determined by the microkjeldahl digestion procedure [39].

## 2.3. Data Analysis

Where individual replicate values were not available, other tests were used. After Loague and Green [40], between the simulated and the measured values, the total difference was calculated as the root mean square error (Smith et al., 1997), RMSE:

$$RMSE = \frac{100}{\bar{O}} \sqrt{\frac{\sum_{i=1}^n (S_i - O_i)^2}{n}} \quad (1)$$

In the following equations,  $O_i$  are the observed values,  $S_i$  are the predicted (simulated) values,  $\bar{O}$  is the mean of the observed data,  $\bar{S}$  is the mean of the predicted (simulated) data, and  $n$  is the number of paired values [28]. The RMSE is a measure of the deviation of the simulated values from observations, and is scaled relative to the units of measurement [41].

$$M = \frac{\sum_{i=1}^n (O_i - S_i)}{n} \quad (2)$$

The nature of the bias was further examined using the mean difference,  $M$  [28]; meanwhile the mean

difference between measured and simulated values gives an indication of the bias in the simulation.

To assess whether simulated values follow the same pattern as measured values, the sample correlation coefficient,  $r$ , can be calculated [28]:

$$r = \frac{\sum_{i=1}^n (O_i - \bar{O})(S_i - \bar{S})}{\sqrt{\sum_{i=1}^n (O_i - \bar{O})^2} \sqrt{\sum_{i=1}^n (S_i - \bar{S})^2}} \quad (3)$$

This statistic can be useful in assessing how well the shape of the simulation matches the shape of the measured data. However, if it is no clear trend in the measured data to give a spread of paired measured and simulated data values, the correlation coefficient is of only limited use in determining how well a model simulates the measured data, meanwhile, an  $r$  value closest to 1 indicates the model matches the pattern of the observations.

There is a soil organic carbon density (SOCD) is the soil organic carbon content, soil bulk density and soil depth which the product of for soil profile is divided into  $n$  layers. The calculation method of soil organic carbon density ( $C_{\text{soil}} \text{ kg m}^{-2}$ )  $C$  is as follows:

$$SOCD = \sum_{i=1}^n (1 - \theta_i\%) \times P_i \times C_i \times T_i / 100 \quad (4)$$

Where SOCD is soil organic carbon density of a profile,  $\theta_i$  is gravel (>2mm) content in horizon  $i$  (%),  $P_i$  is soil bulk density in horizon  $i$  (soil  $\text{cm}^{-3}$ ),  $C_i$  is organic carbon content in horizon  $i$  (soil organic carbon  $\text{g soil kg}^{-1}$ ),  $T_i$  is the thickness of horizon  $i$  (cm), and  $n$  is the numbers of horizons involved [42].

Depths involved in calculation are usually recorded during the field observations with the maximum depth for calculation limited to 20cm. Meanwhile, a GIS was used to link records in the Attributes Database to the Spatial Database based soil samples (using the ArcGIS 9.3). The assignment is done according to the principles of soil parent material identity, soil type identity and similarity. Thereafter, a SOCD ( $\text{kg m}^{-2}$ ) vector map of Manas was compiled by linking SOC density data of soil profiles calculated with the soil spatial database.

$$V = (C_t - C_o) / T \quad (5)$$

Where  $V$  is carbon sequestration rate,  $C_t$  is SOC content in 2041,  $C_o$  is SOC content in 2011 and  $T$  is 30 year.

## 2.4 Model Inputs

In this study, the main input data used the DNDC model include climate, soil, farming management and crop yield (Table 2).

**Table.2** Main input data for running the DNDC model.

Category	Item (Unit)
Climate	Daily maximum and minimum



	temperature(°C), precipitation (mm)
Soil properties	Land-use, Top soil texture, Bulk density, pH, SOC ( $\text{g kg}^{-1}$ ) at surface soil
Farming management and crop yield	crop planting and harvesting dates, the rate and timing of fertilizer application, tillage, weeding, and irrigation

The daily climate data (i.e., maximum and minimum temperature, precipitation in 1980-2010) were collected from China meteorological data sharing service system <http://www.esience.gov.cn>. These datasets are constructed by applying spatial interpolation algorithms to historical climate data from approximately 752 observations across China. There are approximately 56 observations in Xinjiang province. Moreover, input soil properties include the concentrations of organic carbon and total nitrogen, bulk density, clay and sand fraction, and pH in the topsoil to 20 cm depth.

There is a rotation of corn/wheat/cotton in Manas cropland. Corn was seeded during late April to early May for the monocropping system. Spring wheat was seeded in mid-April and winter wheat in late September in the same year. Cotton was seeded in May in this year. Fertilizers were applied at  $\text{NPK}$  and  $\text{K}_2\text{O}$  in Manas cropland (Table 3). Drip irrigation was widespread. Wheat fields were commonly irrigated three to four times, corn fields one or two times, and cotton was commonly irrigated two to three times.

**Table.3** Average annual nutrient input from different source during 1980-2011

Treatment	Chemical fertilizer ( $\text{kg hm}^{-2}$ )			Straw (t $\text{hm}^{-2}$ )
	N	P	K	
NPKS	89.4/216.7 <sup>a</sup>	24.5/50.8	16.9/42.3	4.5/9 <sup>d</sup>

a:annual rate of fertilizer between 1980-1990;

b:annual rate of fertilizer between 1990-2011;

c:wheat strawd:maize straw

## 2.5 Model Validation

The SOC contents in the analysis was obtained from the Second National Soil Survey in 1980, and in Urumqi district, comprising Manas County, was sampled, analyzed and mapped. The sites information for 1980, including cropping systems, soil types, fertilization schemes. Meanwhile, the climate was listed in Figure 2, were also considered in our database.

We validation DNDC to simulate SOC content in the soil using the 1980 year (20 samples, Fig. 3) of our data set. The DNDC was calibrated by testing the full range of possible parameter values for the  $r$ , RMSE,  $M$  and  $R^2$ , which was emphasized in the validation.

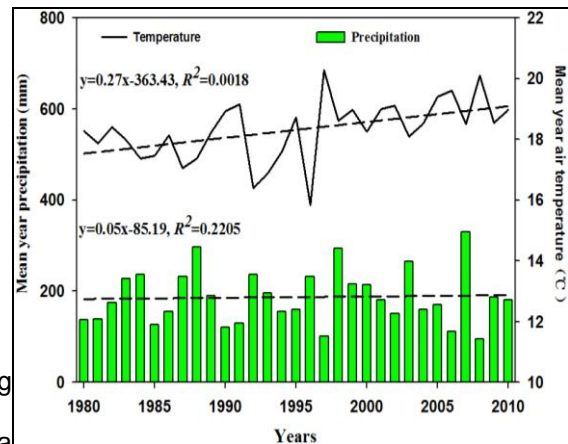


**Fig.2** Mean year precipitation (mm) and mean year air temperature (°C) from 1980 to 2010

Figure 3 showed a change of SOC (1:1 line) during 30 years as simulated by the 9.5DNDC, linear is simulation values ( $\text{g kg}^{-1}$ ) in 2011, and dot is observation values ( $\text{g kg}^{-1}$ ) in 2011. Statistical analysis of the model is conducted by comparing model simulations (Sim) and field observations (Obs) over the course of simulation. Next, we runned our model using forecast the 30 year that SOC content in model validation, we assessed goodness of fitting between simulated and observed SOC content using statistical metrics.

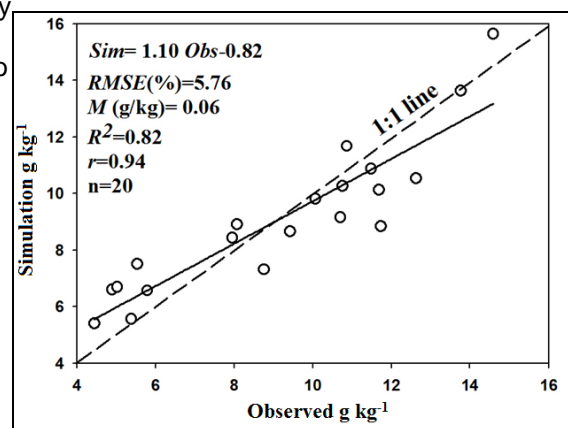


**Fig.3** Modeled vs. observed SOC at the validation sites.

## 3. Results and Analysis

### 3.1 SOC density in Manas

Statistics based on the soil polygon for the SOC ( $\text{kg m}^{-2}$ ) vector map of Manas (Fig.4) show that SOC density in polygons varied dramatically, with the lowest SOC density of  $1.44 \text{ kg m}^{-2}$ , and the highest of  $3.33 \text{ kg m}^{-2}$  in 2011 (Fig.4a). Meanwhile, results of through simulation of 30 year show that the lowest SOC density of  $2.03 \text{ kg m}^{-2}$ , and the highest of  $3.69 \text{ kg m}^{-2}$  in 2041 (Fig.4b). The soil organic carbon content increased range from  $0.38 \text{ g kg}^{-1}$  to  $0.59 \text{ g kg}^{-1}$  during 2011 and 2041 (Fig.4c).

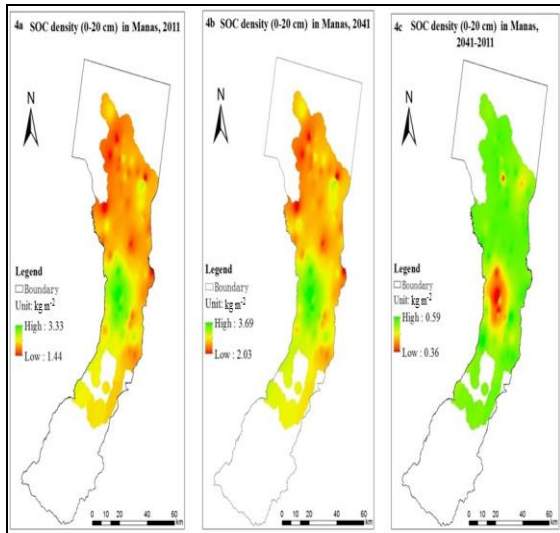


**Fig.4** Map of Soil organic carbon density in Manas (2041-2011).

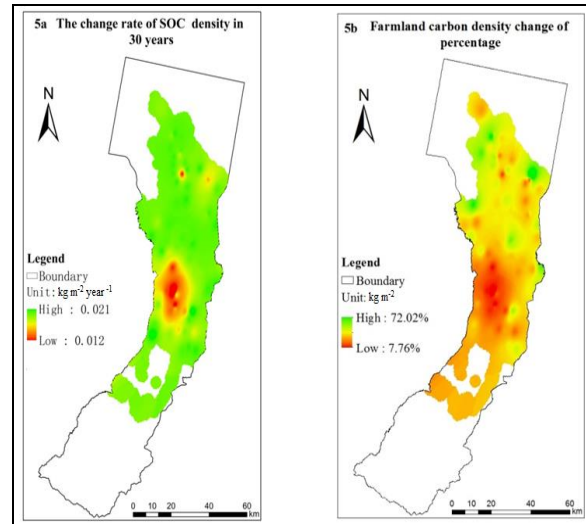


**Fig.5** Manas County farmland soil carbon rate and soil carbon balance in 2011 and 2041 years

Estimates of SOC content and density in China derived from available studies varied greatly. Among published figures, 2009 the analysis of the period from 1998 to 2017 by Liu [43] show that SOC storage could be effectively improved by NPKS in Yujiang country (North, China). Cited from the second general soil survey, the soil organic carbon density and storage of Shandong province (East, China) were estimated by taking soil type as unit. Soil organic carbon density changed from 38.50 to 0.77  $\text{kg m}^{-2}$  with average of 60  $\text{kg m}^{-2}$ , which is lower than the average of China [44]. Meanwhile, Liu's result showed that the SOC density of sandy soil, loess soil in north Shaanxi, and litho soil in Shangluo was the lowest (less than 4  $\text{kg m}^{-2}$ ), whereas the highest SOC density was mainly presented in Guanzhong Plain and Qinling Mountains (up to or even more than 30  $\text{kg m}^{-2}$ ) [45]. The paper (Northwest, China) showed that through DNDC model simulation SOC increased 1.99  $\text{kg}^{-1}$  from 2011 to 2014 year, soil carbon density ranges from 0.012  $\text{kg Cm}^{-2} \text{ yr}$  to 0.021  $\text{kg Cm}^{-2} \text{ yr}$ . Soil carbon sequestration rate ranges from 207  $\text{kg C ha}^{-1} \text{ yr}^{-1}$  to 121  $\text{kg C ha}^{-1} \text{ yr}^{-1}$ , average was 164  $\text{kg C ha}^{-1} \text{ yr}^{-1}$ .

### 3.2 Soil organic Carbon Change of Rate

In accordance with the Manas farmland soil carbon density and fertilizer application show that the relationship between chemical fertilizer and straw returned makes the soil carbon density (2011) increased (Fig. 5a). Meanwhile, the soil carbon density additional rate ranges were 0.012  $\text{kg m}^{-2} \text{ yr}^{-1}$  from 0.021  $\text{kg m}^{-2} \text{ yr}^{-1}$ . In the next 30 years, the maximum rate of the soil carbon density is 207  $\text{kg m}^{-2} \text{ yr}^{-1}$ , the minimum rate is 121  $\text{kg m}^{-2} \text{ yr}^{-1}$ , and the average rate is 164  $\text{kg m}^{-2} \text{ yr}^{-1}$  (Fig. 5b). From 2011 to 2041, soil carbon density ranges from 7.76% to 72.02%, and the Manas farmland soil carbon density shows a trend of increase.

Based on a review of SOC density data from the agricultural literature published before 1960, it has been shown that there have been SOC losses across wide ranges of ecosystems of China [46]. Furthermore when using the DNDC model, it suggested that soil SOC storage has been continuously reducing since the 1950s, and amounting to 70 Tg (1 Tg =  $10^9$  g) since the 1970s [47], when using the DNDC model. These reports have internationally acknowledged, however, dryland ecosystems are particularly sensitive to environmental stresses. Despite their importance to the global carbon cycle, responses of the Central Asian dryland to the rapid climate change in recent decades are still unclear. Using DNDC, a newly developed, spatially explicit process model for dryland ecosystems, a case study was conducted in Xinjiang, a 9154.4  $\text{km}^2$  dry-land cultivation area. The goal was to assess the impacts of future changes on the topsoil regional C dynamics from 2011 to 2041. The results indicated that Xinjiang acted as a C sink of 164  $\text{kg m}^{-2} \text{ yr}^{-1}$ , 93% of which was contributed by increasing NPK+S in the next three decades. The C dynamic overall was dominated by the  $\text{CO}_2$  fertilization effect, which resulted in the addition of soil carbon density from 0.012  $\text{kg m}^{-2} \text{ yr}^{-1}$  to 0.021  $\text{kg m}^{-2} \text{ yr}^{-1}$  with the increase time from 2011 to 2041.

### 3.3 SOC Changed in the Different Types

The C content of the soil in a 10 ha field can be measured precisely, and the error in the measurement defined using replicates, whereas for applications at larger scale, the soil C content is often determined for 1  $\text{km}^2$  grid cells, with the C content estimated from typical or averaged soil C values for the major soil types identified in the cell [48].

The uncertainty due to the structural and input errors can be quantified by evaluating the model at field scale, but using only input drivers that are available at the larger scale. In order to represent the uncertainty,

a range of sites across the whole area to be simulated. SOC is one of the key factors that affect agricultural production, nutrient availability, soil aggregate and the flux of greenhouse gases between land surface and atmosphere [7]. Our results showed that the coincident (indicating a close fit) and associated relationship between the  $\Delta$ SOC and the TN showed negative correlations ( $P < 0.01$ ), the regressive equations for TN was  $y = -2.33x^2 + 2.02x + 1.78$  (Fig.7A). The relationship also in compliance with  $\Delta$ SOC and the TPP ( $P < 0.01$ ), the regressive equations for TP was  $y = -3.72x^2 + 4.01x + 1.08$  (Fig.7B). In addition, the relationship between the  $\Delta$ SOC and sand (%) or  $\Delta$ SOC and clay (%) also showed negative correlations ( $P < 0.05$ ), respectively (Fig.7C and D).  $\Delta$ SOC and SOC ( $P < 0.01$ ) showed regressive equations was  $y = -0.0177x^2 + 0.1715x + 1.81$  (Fig.7E) and  $\Delta$ SOC and SOCD ( $P < 0.01$ ) was  $y = -0.2224x^2 + 0.6083x + 1.81$  (Fig.7F).

Where measurements are replicated, the coincident between simulated and measured values can be expressed as the 'lack of fit' statistic, if a data set is not replicated, the degree of coincidence can instead be determined by calculating the total error as the root mean squared error and the bias as the error as the relative error [40]. The structural and input errors should be calculated separately to allow the source of errors to be understood and reduced, but the combined errors are then used to determine the accuracy of the model simulations at large scale.

The simulated results showed that SOC content increased by 21.68%, 23.49%, 23.56% and 20.76% over that in Gray desert soil, Meadow soil, Solonchaks and Shrubby meadow soils, respectively. In addition, the SOC content also increased by 16.99%, 17.48%, 23.56% and 14.01% over that in Moisture soil, Desert solonchaks and Alluvial soils, respectively. But the SOC content increased by 33.12% and 26.35% in Aeolian sandy soil and irrigated desert soils in the future 30 years, respectively (Fig6).

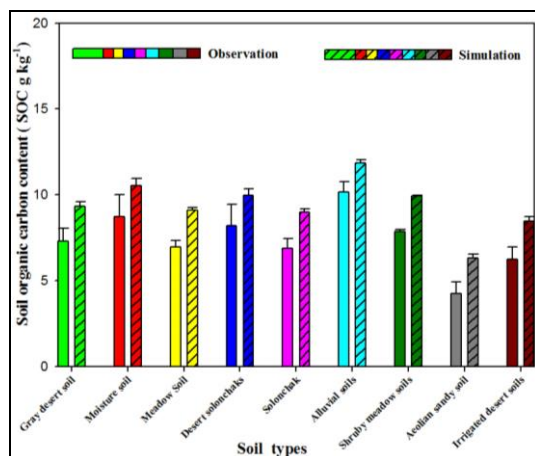


Fig.6 Simulated SOC content by DNDC model from 2011 to 2041 under different soil types

### 3.4 Corresponding of $\Delta$ SOC and the initial value in soil chemical and physical properties

The changes in the SOC concentration ( $\Delta$ SOC) follow a normal distribution with an arithmetic mean of  $1.98 \text{ g kg}^{-1}$ .  $\Delta$ SOC is the different between final and initial measurements (Simulation 2041 and Observation 2011). The SOC content may be mainly attributed to an increase in crop production, residue and manure management [1].

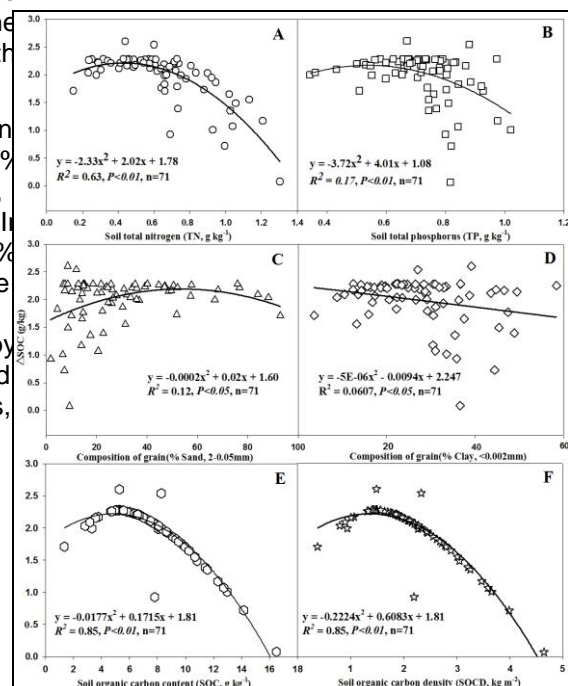


Fig.7 Corresponding of  $\Delta$ SOC and the initial value in soil chemical and physical properties

No-burning harvest systems have several benefits: for instance, higher crop longevity and lower costs for renewing areas; recycling and gradual release of nutrients by straw decomposition; decrease in gas emissions; and less nutrient loss [50]. Increasing soil carbon provides carbon and energy to support microbial activity provides a reservoir of organic N, P and other nutrients for plant productivity and creates more physically cohesive soil to resist soil losses by physical erosion and by protecting occluded organic matter within the larger aggregates [51]. Carbon that enters soil is removed from the atmosphere; any gains in soil carbon mitigate greenhouse gas emissions, with caveats about impacts on the N cycle and N production and the production of CH<sub>4</sub> from the anaerobic decomposition of organic carbon in waterlogged soils [52].



#### 4. Conclusion

Fertilizer application has played an important role in improving the total SOC in the topsoil, demonstrating that NPK+S were better than single chemical fertilizers in ensuring greater accumulation of organic C. This study showed that Manas farmland soil carbon density additional ranges were 0.012 kg m<sup>-2</sup> yr<sup>-1</sup> from 0.021 kg m<sup>-2</sup> yr<sup>-1</sup>. The next 30 years, the maximum rate of the soil carbon density 207 kg m<sup>-2</sup> yr<sup>-1</sup>, the minimum rate of 12 kg m<sup>-2</sup> yr<sup>-1</sup>, the average rate of 164 kg m<sup>-2</sup> yr<sup>-1</sup>. From 2011 to 2041, soil carbon density ranges from 7.76% to 72.02%, the Manas farmland soil carbon density showed a trend of increase. In Northwest China, straw and fertilizer application practices have a positive effect on the soil C sequestration in farmland. Therefore, straw and fertilizer application in dryland farming soil has been promoted as a “win-win strategy” for the sustainable food production and mitigation of greenhouse gas emissions through soil C sequestration. This result has rather significant implications for SOC sequestration potential in semiarid agroecosystems of northwest China.

#### Acknowledgement

This work was supported by Strategic Priority Research Program Climate Change: Carbon Budget and Related Issues of Chinese Academy of Sciences (XDA05050504). We also want to thank Prof. Changsheng Li for helpful suggestions and provision of the DNDC model on the Internet for free use.

#### References

- [1] Cardon ZG, Hungate BA, Cambardella CA, Chapin FC, Field CB, Holland EA, Mooney HA. Contrasting effects of elevated CO<sub>2</sub> on old and new soil carbon pools [J]. *Soil Biology and Biochemistry*, 2001, 33(6): 365-373.
- [2] Follett RF. Soil management concepts and carbon sequestration in cropland soils [J]. *Soil and Tillage Research*, 2001, 61(1): 77-92.
- [3] Lal R. Soil carbon sequestration impacts on global climate change and food security [J]. *Science*, 2004, 304(11): 1623-1627.
- [4] Post WM, Emanuel WR, Zinke PJ. Soil carbon pools and life zones [J]. *Nature*, 1982, 298(1): 156-159.
- [5] Schlesinger WH. Biogeochemistry: an analysis of global change. New York Academic Press. Chuman GE, Janzer HH, Herrick JE. (2002). Soil carbon dynamics and potential carbon sequestration by rangelands [J]. *Environmental Pollution*, 1997, 116(3): 391-396.
- [6] Wang LG, Qiu JJ, Tang HL, Li CS, Ranst EV. Modelling soil organic carbon dynamics in the major agricultural regions of China [J]. *Geoderma*, 2008, 147(3): 47-55.
- [7] Tang JH, Qiu JJ, Eric Van Ranst Li LS. Estimations of soil organic carbon storage in cropland of China based on DNDC model [J]. *Geoderma*, 2006, 134(2): 200-206.
- [8] Lal R. Soil carbon sequestration to mitigate climate change. [J]. *Geoderma*, 2004, 123(1), 1-22.
- [9] Lal R. Carbon management in agricultural soils. 2007 [J]. *Mitig Adapt Strateg Global Change*, 12(2): 303-322.
- [10] Smith P. Agriculture, in Climate Change Mitigation. Contribution of Working Group III to the Fourth Assessment Report of the Intergovernmental Panel on Climate Change, edited by BMetz [M]. Cambridge Univ. Press, Cambridge, New York, 2007, 498-540.
- [11] Sun W, Huang Y, Zhang W, Yu Y. Carbon sequestration and its potential in agricultural soils of china [J]. *Global Biogeochemical Cycles*, 2010, 24(3): 1-12.
- [12] Smith P. Carbon sequestration in croplands: The potential in Europe and the global context [J]. *European Journal of Agronomy*, 2004, 20(1): 229-236.
- [13] Sperow M, Eve M, Paustian K. Potential soil C sequestration on U.S. agricultural soils [J]. *Climate Change*, 2003, 57(3): 319-339.
- [14] Zhang TQ. Study on soil organic carbon storage and changes of agricultural ecosystem in county scale in western Jilin taking Zhenai County as example [M]. 2006 *Jilin university* (in Chinese) <http://book.kongfz.com/21281/180119472/>
- [15] Wang J, Song C, Wang X, Song Y. Changes in labile soil organic carbon fractions in wetland ecosystems along a latitudinal gradient in northeast china [J]. *Catena*, 2012, 96(1): 83-89.
- [16] Tivet F, De MS, Lal R, Borszowske PR, Briedis CD, Santos, JB Séguy L. Soil organic carbon fraction losses upon continuous plowed tillage and its restoration by diverse biomass inputs under no till in sub-tropical and tropical regions of brazil [J]. *Geoderma*, 2013, 209(1): 214-225.
- [17] Shao X, Yang W, Wu M. Seasonal dynamics of soil labile organic carbon and enzyme activities in relation to vegetation types in hangzhou bay tidal flat wetland [J]. *PLoS One*, 2015, 10(11): 1-15.
- [18] Hu L, Wang LG, Qiu JJ, Li CS, Gao MF, Gao CY. Calibration of DNDC model for nitrate leaching from an intensively cultivated region of Northern China. [J]. *Geoderma*, 2014, 223(1): 108-118.
- [19] Molina JAE, Clapp CE, Shaffer MJ, Chichester F W, Larson WE. NCSOIL, a model of nitrogen and carbon transformations in soil: description, calibration and behavior [J]. *Soil Science Society of America Journal*, 1983, 47(1): 85-91.
- [20] Parton WJ, Mosier AR, Ojima DS. Generalized model for N<sub>2</sub> and N<sub>2</sub>O production from nitrification and denitrification [J]. *Global Biogeochemical cycles*, 1996, 10(3): 401-412.

- [21] Jenkinson DS, Hart PBS, Payned JH, Pary LC. Modeling the turnover of organic matter in long term experiments. [J]. *Intecol Bull*, 1987, 15(1): 1-8.
- [22] Hutson JL. LEACHM: model description and users' guide School of Chemistry. Physics and Earth Sciences [M]. *The Flinders University of South Australia, Adelaide*, 2000, 110-114.
- [23] Li C, Frolking S, Frolking TA. A model of nitrous oxide evolution from soil driven by rainfall events: I. Model structure and sensitivity [J]. *Journal of Geophysical Research*, 1992a, 97(9): 9759-9776.
- [24] Li C, Frolking S, Frolking TA. A model of nitrous oxide evolution from soil driven by rainfall events: II Model applications [J]. *Journal of Geophysical Research*, 1992b, 97(9): 9777-9783.
- [25] Li C, Frolking S, Harriss R. Modeling carbon biogeochemistry in agricultural soils [J]. *Global Biogeochemical Cycles*, 1994, 8(1): 237-254.
- [26] Li C, Frolking S, Crocker GJ, Grace PR, Klir J, Martin K, Poulton PR. Simulating trends in soil organic carbon in long term experiments using the DNDC model [J]. *Geoderma*, 1997, 81(1/2): 45-60.
- [27] Li C, Qiu J, Frolking S, Xiang MX, William S, Berrien M, Steve B, Huang Y, Ronald S. Reduced methane emissions from large scale changes in water management of China's rice paddies during 1980-2000 [J]. *Geophysical Research Letters*, 2002, 29(1): 33-37.
- [28] Smith P, Smith JU, Powlson DS. A comparison of the performance of nine soil organic matter models using datasets from seven long term experiments [J]. *Geoderma*, 1997, 81(1): 153-225.
- [29] Han DL, Jia HT, Zhu XP, Xu YM, Han YJ. Using a DNDC model to predict soil organic carbon dynamics in a gray desert soil farmland. [J]. *Resources Science*, 2014, 36(3): 577-583.
- [30] Lioubimtseva E, Cole R, Adams JM, Kapustin G. Impacts of climate and land cover changes in arid lands of Central Asia [J]. *Journal of Arid Environ*, 2005, 62(2): 285-308.
- [31] Pauw ED. Principal biomes of Central Asia. In: Lal, R., Suleimenov, M., Stewart, B.A., Hansen, D.O. & Doraiswami, P. (Eds.), *Climate Change and Terrestrial Carbon Sequestration in Central Asia*. [M]. *Taylor & Francis, London*, 2007, 3-24.
- [32] Lioubimtseva E, Henebry GM. Climate and environmental change in arid Central Asia: impacts, vulnerability, and adaptations [J]. *Journal of Arid Environ*, 2009, 73(1): 963-977.
- [33] Xi C, Bai LL, Qin L, Jun LL, Saparnova A. Spatiotemporal pattern and changes of evapotranspiration in arid Central Asia and Xinjiang of China [J]. *Journal of Arid Land*, 2012, 4(1): 105-112.
- [34] Gong Y, Hu Y, Fang F, Liu Y, Li K, Zhang G. Carbon storage and vertical distribution in three shrubland communities in Gurbantunggut desert, Uygur autonomous region of Xinjiang, Northwest China [J]. *Chinese Geographical Science*, 2012, 22(5): 541-549.
- [35] Li C, Zhang C, Luo G, Chen X. Modeling the carbon dynamics of the dryland ecosystems in Xinjiang, China from 1981 to 2007: the spatiotemporal patterns and climate controls [J]. *Ecological Modelling*, 2013, 267(10): 148-157.
- [36] Nelson DW, Sommers LE. Total carbon, organic carbon, and organic matter. In: A.L. Page, R.H. Miller, & D.R. Keeney, editors, *Methods of soil analysis. Part 2. 2nd ed* [M]. *ASA and SSSA*, 1982, 537-577.
- [37] Blake GR, Hartage KH. Bulk density. In: A. Klute, editor, *Methods of Soil Analysis. Part 1* [M]. *ASA and SSSA*, 1986, 363-375.
- [38] Du JL, Jin MG, Ouyang ZP. Soil Particle Size Analysis of Yanqi Basin [J]. *Geological Science and Technology Information*, 2008, 27(4): 91-94 (In Chinese).
- [39] Bremner JM, Mulvaney CS. Nitrogen total. *Agron Monogr* 9 [M]. *ASA and SSSA*, 1982, 595-624.
- [40] Loague K, Green, RE. Statistical and graphical methods for evaluating solute transport models: overview and application [J]. *Journal of Contaminat Hydrology*, 1991, 7(2): 51-73.
- [41] Christina T, Mark B. David, Laurie E. Li CS. Application of the DNDC model to till drained Illinois agroecosystems: model calibration, validation, and uncertainty analysis [J]. *Nutrient Cycling in Agroecosystems*, 2007, 78(1): 51-63.
- [42] Yu DS, Shi XZ, Wang HJ, Su WX, Chen JM, Liu QH, Zhao YC. Regional patterns of soil organic carbon stocks in China [J]. *Journal of Environmental Management*, 2007, 85(3): 680-689.
- [43] Liu Q, Sun B, Xie XL, Li ZP. The spatial temporal dynamic change and simulation of County-scale paddy soil organic carbon in red soil hilly region. [J]. *Acta Pedologica Sinica*, 2009, 46(6): 1059-1066 (In Chinese).
- [44] Zhang BH, Zhang JP, Liu ZT, Xue T. Soil Organic Carbon Density and Storage Estimate of Shandong Province [J]. *Chinese Journal of Soil Science*. 2006, 39(5): 1030-1033.
- [45] Liu J, Chang QR, Chen T, Liu, MY, Qi YB. Spatial Distribution Characteristics and Estimation of Soil Organic Carbon Density and Storage in Shanxi Province, in China [J]. *Chinese Journal of Soil Science*, 2012, 43(3): 566-661 (In Chinese).
- [46] Lindert PH, Lu I, Wu W. Trends in the soil chemistry of South China since the 1930s [J]. *Soil Science*, 1996, 161(3): 329-342.



- [47] Li CS. Loss of soil carbon threatens Chinese agriculture: A comparison on agroecosystem carbon pool in China and the U.S[J]. *Quaternary Sciences*, 2000 20(4): 345-350.
- [48] Barto EK, Alt F, Oelmann Y, Wilcke W, Rillig, MC. Contributions of biotic and abiotic factors to soil aggregation across a land use gradient [J]. *Soil Biology and Biochemistry*, 2010, 42(12): 2316-2324.
- [49] Smith JMBJL, Bolton VLBH. Priming effect and C storage in semiarid no-till spring crop rotations. [J] *Canadian Journal of Soil Science*, 2003 37(1): 237-244.
- [50] Canellas LP, Berner PG, Silva SG, Barros EM, Santos GA. Frações da matéria orgânica em solos de uma toposequência no estado do Rio de Janeiro. *Pesquisa [J]. Agropecuária Brasileira*, 2000 35(3): 133-143.
- [51] Morrissey EM, Berrier DJ, Neubauer SC, Franklin RB. Using microbial communities and extracellular enzymes to link soil organic matter characteristics to greenhouse gas production in a tidal freshwater wetland [J]. *Biogeochemistry*, 2014 117(2): 473-490.
- [52] Rhodes CJ. Feeding and healing the world: Through regenerative agriculture and permaculture [J] *Science Progress*, 2012 95(3): 345-348.